Genomic profiling of a metastatic anaplastic melanocytic neuroectodermal tumor arising from a mature thymic teratoma as part of a mediastinal germ cell tumor

Sylvain Mayeur, Benoît Lhermitte, Justine Gantzer, Anne Molitor, Tristan Stemmelen, Sébastien Meyer, Aline Kolmer, Jean-Emmanuel Kurtz, Seiamak Bahram, Raphaël Carapito

COLD SPRING HARBOR
Molecular Case Studies

RESEARCH REPORT

Genomic profiling of a metastatic anaplastic melanocytic neuroectodermal tumor arising from a mature thymic teratoma as part of a mediastinal germ cell tumor

Sylvain Mayeur,[1,2] Benoit Lhermitte,[2] Justine Gantzer,[3] Anne Molitor,[1] Tristan Stemmelen,[1] Sébastien Meyer,[1] Aline Kolmer,[1] Jean-Emmanuel Kurtz,[3] Seiamak Bahram,[1,4,5] and Raphael Carapito[1,4,5]

[1]Laboratoire d'ImmunoRhumatologie Moléculaire, Plateforme GENOMAX, INSERM UMR_S 1109, Faculté de Médecine, Fédération Hospitalo-Universitaire OMICARE, ITI TRANSPLANTEX NG, Strasbourg Federation of Translational Medicine (FMTS), Strasbourg University, Strasbourg 67091, France; [2]Department of Pathology, Strasbourg University Hospitals, Strasbourg 67200, France; [3]Pôle d'oncologie médico-chirurgicale et d'hématologie, ICANS-Europe, Strasbourg 67200, France; [4]Laboratoire d'Immunologie, Plateau Technique de Biologie, Pôle de Biologie, Nouvel Hôpital Civil, Strasbourg 67091, France

Abstract Following chemotherapy, a mediastinal germ cell tumor can lead to a mature teratoma that is composed of tissues derived from all three germ layers. Although teratoma is usually curable, in rare cases it can give rise to various somatic tumors and exceptionally it undergoes melanocytic neuroectodermal tumor (MNT) transformation, a process that is not well-described. We report a patient with a postchemotherapy thymic teratoma associated with an MNT component who, 10 years later, additionally presented a vertebral metastasis corresponding to an anaplastic MNT. Using exome sequencing of the mature teratoma, the MNT and its metastatic vertebral anaplastic MNT components, we identified 19 somatic mutations shared by at least two components. Six mutations were common to all three components, and three of them were located in the known cancer-related genes *KRAS* (p.E63K), *TP53* (p.P222X), and *POLQ* (p.S447P). Gene set enrichment analysis revealed that the melanoma tumorigenesis pathway was enriched in mutated genes including the four major driver genes *KRAS*, *TP53*, *ERBB4*, and *KDR*, indicating that these genes may be involved in the development of the anaplastic MNT transformation of the teratoma. To our knowledge, this is the first molecular study realized on MNT. Understanding the clinicopathological and molecular characteristics of these tumors is essential to better understand their development and to improve therapeutics.

[Supplemental material is available for this article.]

Corresponding authors: siamak@unistra.fr; carapito@unistra.fr

Ontology term: neoplasm of the thymus

Published by Cold Spring Harbor Laboratory Press

doi:10.1101/mcs.a006257

INTRODUCTION

Mediastinal germ cell tumors (GCTs) represent a heterogeneous group of neoplasms originating from primitive germs left in the mediastinum during embryogenesis. They can be

[5]These authors contributed equally to this work.

classified as seminomatous or nonseminomatous tumors (Marx et al. 2022). Their prognosis depends on tumor histology, stage, and serum markers. Nonseminomatous neoplasms represent up to 85% of mediastinal GCTs including teratoma (Pini and Colecchia 2022). Their treatment requires chemotherapy followed by surgical resection of the residual tumor (Albany and Einhorn 2013). This systemic treatment can select the teratomatous component present in the mediastinal GCT, leading to a residual postchemotherapy mature teratoma component at the initial and/or metastatic locations of the GCT (Green et al. 2021).

Teratoma is a GCT defined as a neoplasm originating from pluripotent cells that form differentiated somatic-type tissues, which may be either mature, immature, or both (Marx et al. 2022). The majority of teratomas carry mature tissues and have a favorable prognosis. Immature teratomas represent only 4% of mediastinal teratomas but have a malignant potential that correlates with the proportion of immature tissues (Dulmet et al. 1993; Moran and Suster 1997; De Backer et al. 2008). In rare cases, a part of the mature teratoma may undergo a somatic transformation into a malignant nongerminal cell tumor that is equivalent to a somatic malignancy (Motzer et al. 1998). A wide variety of somatic-malignancy transformations have been described but the most frequent ones are adenocarcinoma, primitive neuroectodermal tumors, and rhabdomyosarcoma (Motzer et al. 1998; Ryu et al. 2013; Marx et al. 2022). In addition, exceptional cases of melanocytic neuroectodermal transformation (MNT) have been reported (Misugi et al. 1965; Hameed and Burslem 1970; Tobo et al. 1981; King et al. 1985; Anagnostaki et al. 1992; Vajtai et al. 2000). MNTs are extremely rare, yet rapidly growing, benign tumors consisting of a biphasic population of small neuroblast-like and larger melanin-producing epithelioid cells. Children are mostly affected by MNTs that occur in the head and neck region (Almomani and Rentea 2022), but extracranial locations have also been reported (Styczewska et al. 2021). Nearly 500 cases have already been reported but only six were linked to a teratoma (Misugi et al. 1965; Hameed and Burslem 1970; Tobo et al. 1981; King et al. 1985; Anagnostaki et al. 1992; Vajtai et al. 2000).

The presence of somatic mutations induced by genomic instability of a precursor cell has been proposed to be the trigger of the development of GCTs and in particular teratoma (Feldman et al. 2014; Taylor-Weiner et al. 2016). Similar molecular events might contribute to the development of the malignant component. Although studying these cases is an opportunity to better understand the mechanisms that are involved in the malignant transformation, such studies are sparse in the literature, mainly descriptive and lacking molecular data. This caveat is mainly due to the rarity but also to the technical challenges of selecting and reliably analyzing the various neoplastic components.

Here, we report an extremely rare case of a patient who presented with a mediastinal GCT presenting as a mature teratoma after chemotherapy with an MNT component and secondly developed vertebral metastatic localization with an anaplastic transformation of the MNT that was histologically close to a malignant melanoma. Besides clinical and pathological evaluation, we aimed to characterize the molecular events associated with the teratoma and its melanocytic transformation using both targeted gene-panel and exome sequencing.

RESULTS

Clinical Presentation and Family History

A Caucasian male born with anal imperforation and bilateral cryptorchidism was referred at 26 yr of age for dyspnea. No pathogenic germline variant in known genes of cryptorchidism, congenital anorectal malformations, and cancer susceptibility genes were identified. Physical and radiological examination showed a mediastinal tumor measuring 9 cm × 8 cm × 7 cm (Fig. 1A) metastatic to the pleura, liver, and an isolated brain metastasis. Initial assessment showed α-fetoprotein at 40 μg/L, β-human chorionic gonadotropin at

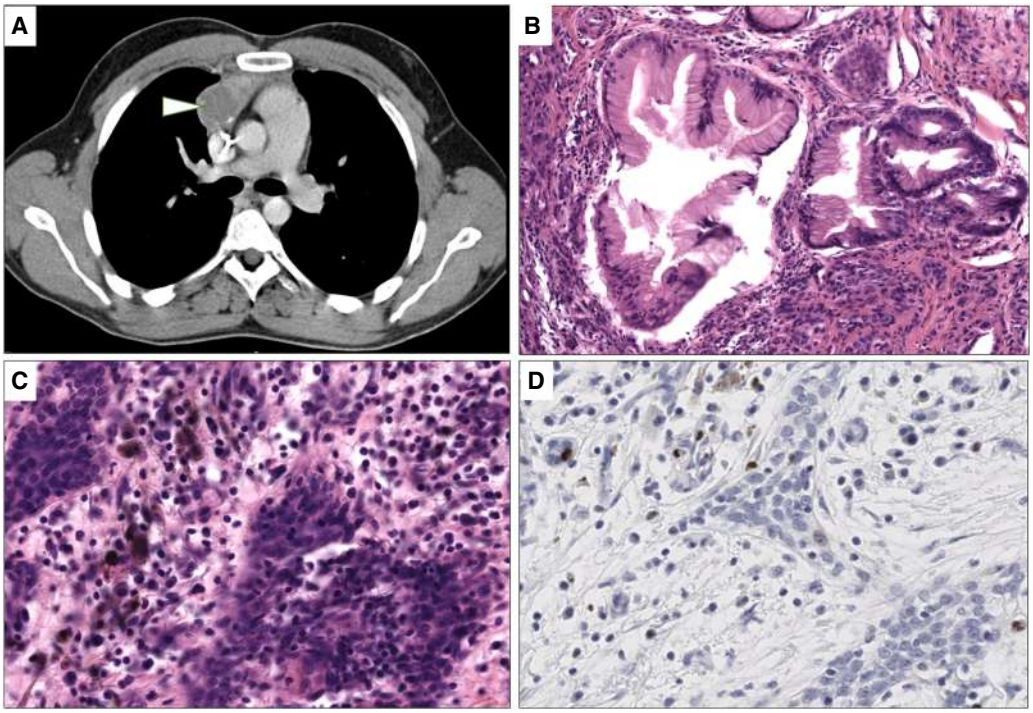

Figure 1. Radiological and histological features of mediastinal lesion. (*A*) Computed tomography scan imaging showing presence of hypodense lesion of the right anterior mediastinum (arrowhead). (*B*) Mature teratoma with mature fundic differentiation without cytologic atypia and representing 70% of the viable tumor (10×, hematoxylin and eosin [H&E] stain). (*C*) Melanocytic neuroectodermal transformation (MNT) component with one pleiomorphic cell population containing intracytoplasmic melanin pigments and a second small basophilic cell population (40×, H&E stain). (*D*) Ki67 immunohistochemistry showing a low proliferation index of the MNT component. Brown nuclear stain highlights a Ki67-positive tumor cell and granular cytoplasmic brown corresponds to melanin pigments.

61114 U/L, and lactate dehydrogenase at 1100 U/L, diagnosing nonseminomatous germ-cell cancer. He received several lines of chemotherapy including BEP (bleomycin, etoposide, cisplatin), T (paclitaxel)-BEP/oxaliplatin, and cisplatin-ifosfamide because of insufficient marker response. Five months later, he underwent brain surgery for the brain metastasis, which was partially removed, showing teratoma. He was treated with six cycles of doxorubicin, cyclophosphamide, and methotrexate followed by whole-brain radiation therapy and was considered as in complete remission. A recurrence of the occipital metastasis was removed at 27 yr of age and revealed reactional and benign fibromatous gliosis corresponding to post-treatment remodeling. Five months later, radical thymic compartment resection was performed. Microscopic examination revealed a tumoral mass composed of 50% fibro-necrotic remodeling. The viable territory was composed of 70% fundic and intestinal glandular mature teratoma (Fig. 1B), 25% MNT (Fig. 1C), and 5% angiosarcomatous component. MNT tumoral fraction was composed of pleiomorphic large cells with vesicular nuclei and intracytoplasmic melanin pigment inclusions and small round cells with little basophilic cytoplasm and small dark nuclei. Immunohistochemistry on MNT showed a strong expression of PS-100 as well as the melanocytic markers SOX10, Melan-A, and HMB45. MNT was negative for glypican 3, bHCG, synaptophysin, panKeratin AE1/AE3, and SALL4. The Ki67 proliferative index was low (<1%) (Fig. 1D)

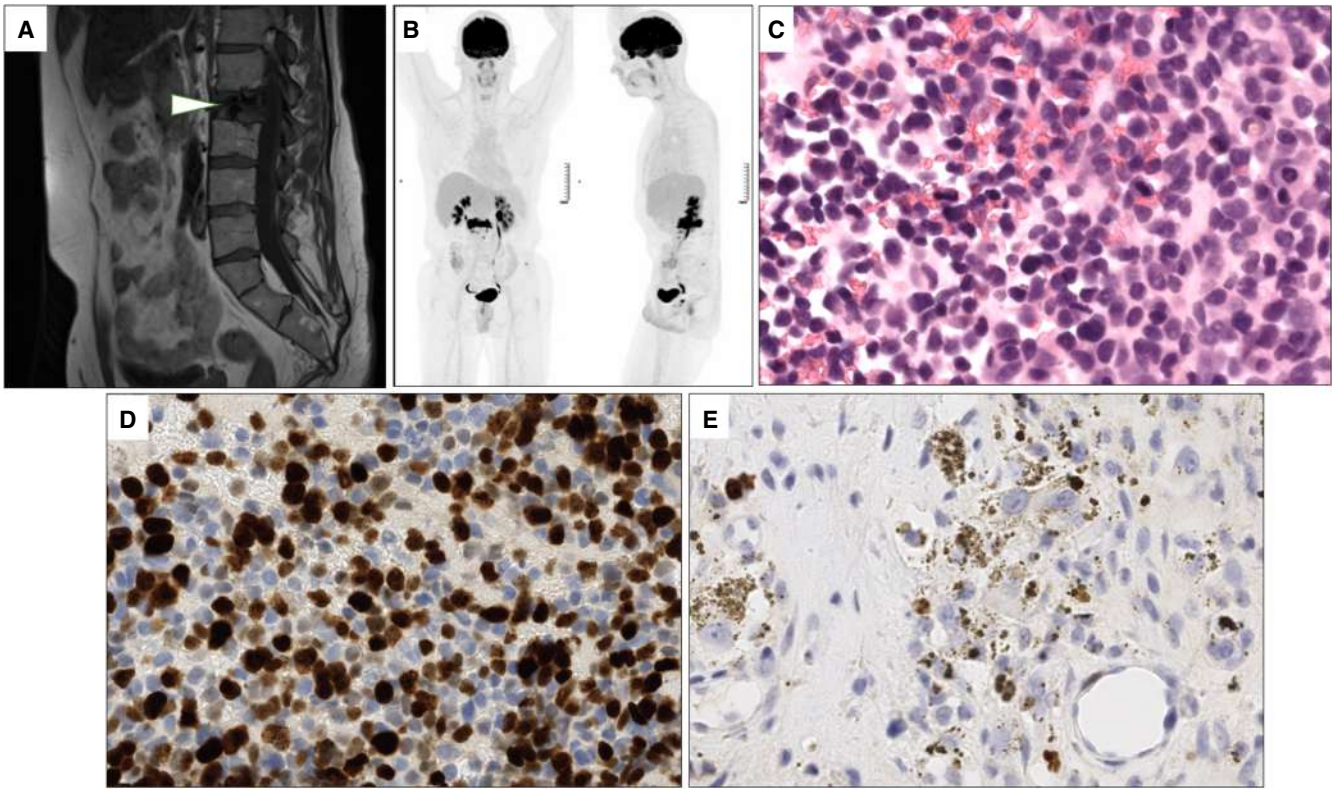

Figure 2. Radiological and histological features of the vertebral metastases. (*A*) T1-weighted magnetic resonance image of the hypointense L2 spinal metastatic lesion (arrowhead). (*B*) 18F-fluorodeoxyglucose-positron emission tomography-computed tomography (18F-FDG-PET/CT) scan imaging revealing a hypermetabolism of the L2 spinal metastasis. (*C*) Microscopic examination of the pretreatment vertebral metastasis corresponding to an anaplastic melanocytic neuroectodermal transformation (MNT). Cells are pleiomorphic and numerous mitoses are visible (40×, hematoxylin and eosin [H&E] stain). (*D*) Ki67 immunohistochemistry in the same pretreatment vertebral biopsy showing an important proliferative index of the tumoral cells. Brown nuclear staining highlights Ki67-positive tumor cells and granular cytoplasmic brown corresponds to melanin pigments. (*E*) Ki67 immunohistochemistry of the post-therapy vertebral cell highlighting the presence of a residual MNT component with a lower proliferative index.

At age 28, standard follow-up showed an osteolytic lesion of L2 vertebra (Fig. 2A). Multiple biopsy samples from this lesion showed the presence of mesenchymatous tissue corresponding immature teratoma remnants with a low (1%) Ki67 index.

The patient remained in complete remission until age 38, when a fluorodeoxyglucose-positron emission tomography (FDG-PET) scan showed an increased L2 glucose uptake (Fig. 2B). Biopsy revealed a proliferation consisting of small-sized cells with chromatic nuclei and faint cytoplasm. Numerous mitoses were found with a Ki67 proliferative index of 50% (Fig. 2C,D). The lesion was histologically close to a malignant melanoma, expressed the melanocytic markers HMB45 and Melan-A and was classified as an anaplastic transformation of the MNT. The patient received another chemotherapy line with carboplatin and etoposide targeting the immature pathological features of the tumor were done and complete surgical L2 resection was performed. Microscopical analysis showed an important fibro-necrotic post-treatment remodeling with presence of 10% neoplastic proliferation close to the original MNT described above. The Ki67 proliferative index was 1% but reached 10% focally (Fig. 2E).

Radiological evaluation performed at age 39 showed locoregional retroperitoneal lymph node evolution leading to an immunotherapy initiation (ipilimumab–nivolumab). To date, the patient is still alive with poor therapeutic response.

Genomic Analyses

An oncogenetic assessment including 26 target genes was carried out only on the post-treatment proliferative MNT component of the vertebral metastasis. This analysis revealed the presence of a p.E63K mutation in KRAS (variant allele frequency [VAF] 37.5% and 38% in targeted panel and exome, respectively). Then, we performed exome sequencing in order to identify somatic mutations specific of each neoplastic component and to further analyze their similarities. We analyzed the germline thymic sample, the mature teratoma, and the MNT components that were derived from the radical thymic compartment resection (at age 27 yr) and the metastatic anaplastic MNT that was derived from the vertebral metastasis (at age 37 yr). The sequencing of the mature teratoma, MNT, metastatic MNT, and matched germline thymic samples resulted in an average depth of coverage of 317.5, 405, 194.4, and 172, respectively. The three components shared six mutations, and 13 mutations were present in at least two components. Among the variants shared by the three components, three are modifying amino acids in proteins known to be involved in oncogenesis. The p.E63K mutation in KRAS is one of the mutations that had previously been described in the targeted gene-panel sequencing. The two others are p.P222X in TP53 and p.S447P in POLQ (Table 1; Fig. 3A; Supplemental Table S1). Other variants in genes potentially involved in oncogenesis were also identified in each component (Fig. 3A). However, none of them are localized in codons that are already known to impact oncogenesis. Using gene set enrichment analysis (GSEA), we observed specific mutational profiles in genes involved in the "Melanoma," "Epithelial to mesenchymal transition in colorectal cancer," "Regulation of actin cytoskeleton," "Chemokine signaling pathway," and "Folate metabolism" pathways (Fig. 3B; Supplemental Table S2). Interestingly, the "Melanoma" pathway is the most enriched one and contains four genes that are all implicated in oncogenesis (*KRAS*, *TP53*, *ERBB4*, and *KDR*).

DISCUSSION

We report a rare case of a postchemotherapy mediastinum teratoma leading to a somatic-type malignant transformation toward MNT and anaplastic MNT that was histologically close to a malignant melanoma (Supplemental Fig. S1).

MNT is a rare tumor particularly affecting children of <1 yr of age and localized in the craniofacial region in 90% of cases (Barrett et al. 2002). To our knowledge, only six cases of MNT have been described in a context of teratoma. Three of them were related to ovarian teratoma (Hameed and Burslem 1970; King et al. 1985; Vajtai et al. 2000), two arose from mediastinal teratoma (Misugi et al. 1965; Anagnostaki et al. 1992), and one from the sellar region (Tobo et al. 1981). These patients are often older than those with classical MNT. Although MNTs are generally benign, three of the six previously described cases were very aggressive and metastatic (Hameed and Burslem 1970; King et al. 1985; Anagnostaki et al. 1992). Altogether, these data suggest that in the context of teratoma, the mechanism of tumor development is different from classical MNT.

The absence of anatomopathological examination of the primitive tumor before neoadjuvant therapy did not allow us to clearly conclude about the origin of the teratoma component. It may have been initially present in the GCT and selected by the chemotherapy or it may result from the chemotherapy-induced maturation of immature cells of the GCT. Although the etiopathogenesis of teratoma is not fully understood, it has been suggested

Table 1. List of coding somatic variants in census genes according to the COSMIC database

Chr.	Pos.	Ref.	Alt.	Type of variant	Gene symbol	HGVSp short	SIFT	PolyPhen	rsID/Cosmic ID	Cosmic database information		Cancer type observation in COSMIC Database	Tera-toma (VAF %)	MNT (VAF %)	Ana-plastic MNT (VAF %)
										Census gene	Role in cancer				
1	7723485	G	A	Missense	*CAMTA1*	p.R293Q	T	Prob. dam.	rs753954585	Tier 1	Tumor suppresor, fusion	Large intestine adenocarcinoma, malignant melanoma	9.26	–	–
1	17965150	C	T	Missense	*ARHGEF10L*	p.R416C	D	Prob. dam.	rs1304791222	Tier 2	Tumor suppresor	–	–	8.77	–
1	205628612	C	T	Missense	*SLC45A3*	p.R471H	T	Benign	rs765881137/ COSM6887586	Tier 1	Fusion	–	–	8.47	–
2	46605084	C	T	Missense	*EPAS1*	p.P434L	D	Prob. dam.	rs745357489	Tier 1	Oncogene, tumor suppressor	–	9.62	–	–
2	212286781	G	A	Missense	*ERBB4*	p.A972V	T	Benign	–	Tier 1	Oncogene, tumor suppressor	–	–	–	12.2
3	47165718	C	A	Missense and NMD transcript	*SETD2*	p.R8S	D	Prob. dam.	–	Tier 1	Tumor suppresor	–	–	12.82	–
3	121238847	A	G	Missense	*POLQ*	p.S447P	D	Poss. dam.	–	Tier 1	Oncogene, tumor suppressor	–	25.68	8.57	23.53
4	55948198	G	A	Missense	*KDR*	p.T1258M	D	Prob. dam.	rs147627339	Tier 1	Oncogene	Large intestine adenocarcinoma, pancreatic ductal carcinoma	–	–	20.71
4	88035579	C	T	Missense	*AFF1*	p.P525S	T	Prob. dam.	–	Tier 1	Fusion	–	13.89	–	–
5	180058713	C	T	Missense	*FLT4*	p.D42N	T	Benign	rs777334601	Tier 1	Oncogene	–	–	10.14	–
6	150001575	C	A	Missense	*LATS1*	p.A677S	T	Benign	–	Tier 1	Tumor suppresor	–	–	–	11.36
7	50468251	G	A	Missense	*IKZF1*	p.G496S	D	Prob. dam.	rs548117828	Tier 1	Tumor suppresor, fusion	–	–	13.64	–
7	98579527	C	T	Missense	*TRRAP*	p.R2899C	D	Prob. dam.	rs1792941314	Tier 1	Oncogene	–	10.58	–	–
7	127326707	G	A	Missense	*SND1*	p.R40H	T	Benign	rs773076395/ COSM6786017	Tier 1	Oncogene, Fusion	Large intestine adenocarcinoma	–	11.76	–
8	101730335	C	A	Missense	*PABPC1*	p.G123C	D	Prob. dam.	rs755674364	Tier 2	Oncogene, tumor suppressor	Astrocytoma, acute myeloid leukemia, colon adenocarcinoma, squamous cell carcinoma	–	–	11.67
11	46329469	C	T	Missense	*CREB3L1*	p.S145L	T	Prob. dam.	rs746245139	Tier 1	Tumor suppresor, fusion	–	6.33	–	–
11	118629536	C	T	Missense	*DDX6*	p.A314T	T	Prob. dam.	–	Tier 1	Oncogene, fusion	–	9.09	–	–
12	22797153	C	T	Missense	*ETNK1*	p.S231L	D	Benign	rs764046781	Tier 1	Tumor suppresor	–	–	10.91	–
12	25380271	C	T	Missense	*KRAS*	p.E63K	D	Prob. dam.	COSM27159	Tier 1	Oncogene	Malignant melanoma, colon adenocarcinoma, bladder carcinoma, carcinoid endocrine tumour, seminoma, acute lymphoblastic leukaemia	11.32	10.07	38.04
12	48373317	G	A	Missense	*COL2A1*	p.V835I	D	Prob. dam.	rs121912882	Tier 1	Fusion	–	10.71	–	–
15	90628058	C	T	Missense	*IDH2*	p.G421S	Dlc	Prob. dam.	rs1023592505	Tier 1	Oncogene	Rectum adenocarcinoma, ovary mixed adenosquamous carcinoma	–	10.42	–

(*Continued on next page.*)

Table 1. (*Continued*)

Chr.	Pos.	Ref.	Alt.	Type of variant	Gene symbol	HGVSp short	SIFT	PolyPhen	rsID/Cosmic ID	Cosmic database information		Cancer type observation in COSMIC Database	Tera-toma (VAF %)	MNT (VAF %)	Ana-plastic MNT (VAF %)
										Census gene	Role in cancer				
15	93524121	G	A	Missense	*CHD2*	p.G985R	D	Prob. dam.	.	Tier 2	Tumor suppresor	–	–	–	11.49
16	3778563	C	T	Missense	*CREBBP*	p.G2162E	Dlc	Poss. dam.	rs1401593486	Tier 1	Oncogene, tumor suppressor, fusion	–	11.63	–	–
16	3808047	G	T	Missense and splice region	*CREBBP*	p.D1124E	D	Poss. dam.	–	Tier 1	Oncogene, tumor suppressor, fusion	–	–	–	17.95
17	5268516	G	A	Missense	*RABEP1*	p.E590K	D	Benign	rs757825581	Tier 1	Fusion	Endometrioid carcinoma	8.93	–	–
17	7578183	CG	C	Frameshift	*TP53*	p.P222X	–	–	rs1567551073	Tier 1	Oncogene, tumor suppressor, fusion	–	44.83	32	42.86
17	30325720	G	A	Missense	*SUZ12*	p.V640I	T	Poss. dam.	–	Tier 1	Oncogene, Tumor suppressor, Fusion	–	17.65	–	–
X	48123289	G	A	Missense	*SSX1*	p.D135N	T	Poss. dam.	rs782680032	Tier 1	Oncogene, fusion	Astrocytoma, papillary renal cell carcinoma	–	15.79	–

Gene symbols are based on the HUGO Gene Nomenclature Committee (HGNC). All variants were validated by visualization with the Integrative Genomics Viewer (IGV).
(Chr.) Chromosome, (Pos.) genomic position according to genome version hg19 (GRCh37), (Ref.) reference base, (Alt.) alternative base, (MNT) melanocytic neuroectodermal tumor, (SIFT T) tolerated variant as predicted by the SIFT (Sorting Intolerant From Tolerant) program (https://sift.bii.a-star.edu.sg/), (SIFT D) deleterious variant as predicted by the SIFT program, (SIFT Dlc.) deleterious low confidence as predicted by the SIFT program, (Polyphen Prob. dam.) probably damaging variant as predicted by the PolyPhen program (http://genetics.bwh.harvard.edu/pph2/), (Polyphen Poss. dam.) possibly damaging variant as predicted by the PolyPhen, (rsID) rs identification number, (VAF) variant allele frequency.

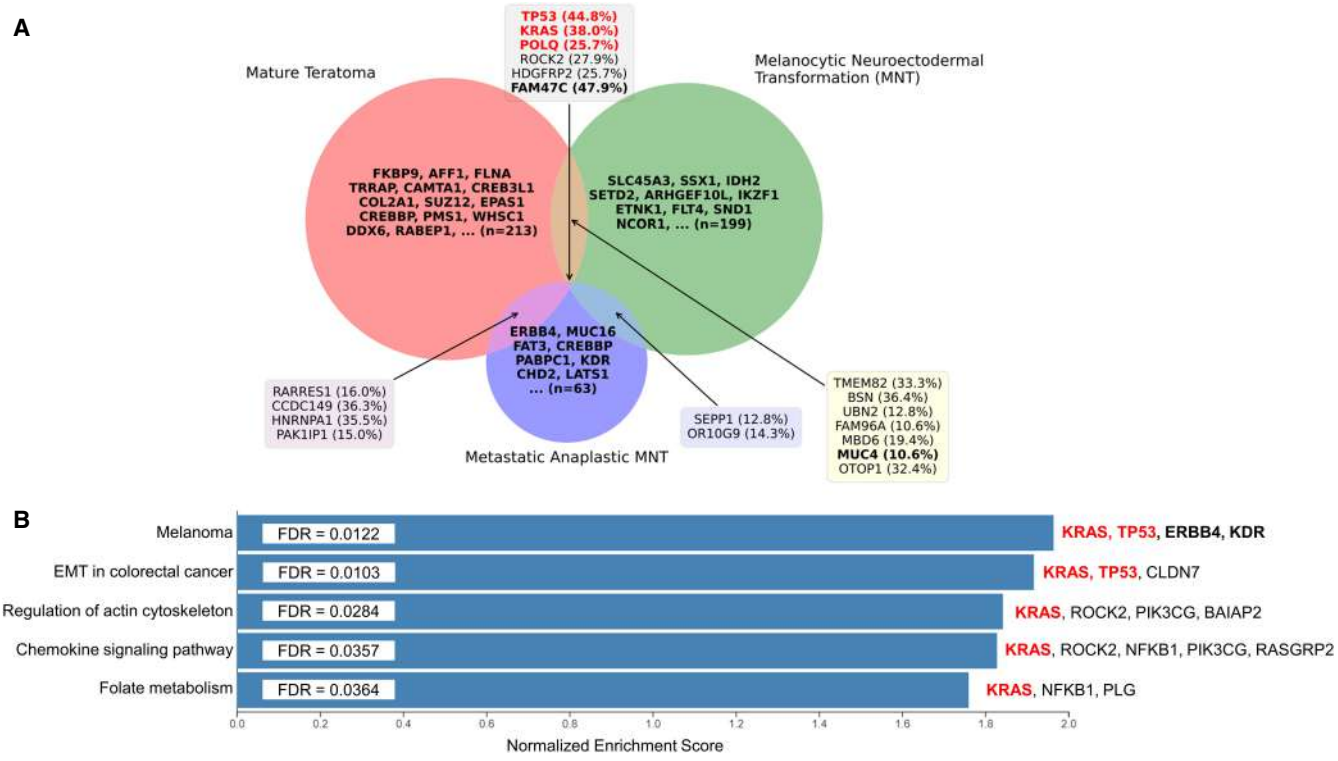

Figure 3. Somatic mutation profile of the mature teratoma, melanocytic neuroectodermal transformation (MNT), and metastatic anaplastic MNT. (*A*) Venn diagram analysis of the three different components showing six mutations shared by the three different component and 13 mutations common to at least two components. Variant allele frequencies are indicated in brackets. (*B*) Gene set enrichment analysis (GSEA) using Wikipathway reveals a significant normalized enrichment score in the melanoma pathway. For *A* and *B*, genes involved in oncogenesis according to the COSMIC database are indicated in bold. The oncogenic specific mutations appear in red.

that it originates from a germ cell precursor that erroneously stopped in midline migration during embryogenesis (Ronchi et al. 2019). Because of the high expression of KIT ligands that are implicated in germ cell proliferation, the thymus might be the preferential site for this germ cell precursor arrest (Oosterhuis et al. 2007; Ronchi et al. 2019). In some cases, this precursor may lead to a germ cell neoplasia which is a type II GCT precursor and then lead to the different subtypes including teratoma (Fichtner et al. 2021).

Teratoma seems to share genetic characteristics with other types of GCT. As the other type II GCT, adult teratoma are characterized by gain of Chromosome 12p or an isochromosome 12p (Lee et al. 2019; Fichtner et al. 2021). During the transition from precursor to the invasive component, acquisition of additional genetic alterations in genes involved in germ cell tumorigenesis and proto-oncogenes have been reported (Blanco and Tirado 2018; Fichtner et al. 2021). As the different lines of chemotherapy administered to the patient including cisplatin, etoposide, and paclitaxel have been described in the development of postexposure secondary neoplasms, mainly acute myeloid leukemia (Larson 2009; Smith et al. 2011), it is possible that the malignant transformation of teratoma is chemotherapy-induced.

Exome sequencing on the postchemotherapy mature thymic teratoma, the MNT, and its metastatic vertebral anaplastic MNT revealed six common mutations, among which three are located in known oncogenic factors or tumor suppressor genes. The first one is p.P222X

in the R175–R282 hotspot region of the DNA binding domain of TP53, which is mutated in close to 50% of all human solid cancers (Chiang et al. 2021; Marei et al. 2021). According to a recent genomic study on intracranial teratomas, TP53 is not among the most frequently mutated genes (Zhang et al. 2022). Nevertheless, this study showed that the TP53 signaling pathway is affected in 18% of cases and that TP53 mutations might be associated with poor prognosis. The role of TP53 alterations on the development of teratoma and malignant somatic transformation is, however, not well-understood (Zhang et al. 2022). It has also been shown that TP53 mutations play a crucial role in squamous cell carcinoma arising from ovarian mature cystic teratoma (Cooke et al. 2017; Tamura et al. 2020, 2023). Finally, in mediastinum, GCT with TP53 mutation have a worsening response to platinum-based chemotherapy (Timmerman et al. 2021). The second mutation is the p.E63K mutation of KRAS, which is part of the curated mutation list of the COSMIC database and has been reported in genital tract, pancreas, lymphoid tissue, large intestine, and thyroid neoplasms (Bamford et al. 2004). KRAS mutation seems to be the most common somatic alteration observed in GCT (Taylor-Weiner et al. 2016). Interestingly, the p.E63K mutation has also been described in three cases of extragonadal seminoma, a subtype of GCT, in a case of primitive neuroectodermal tumor-medulloblastoma and in a case of malignant lymphoma (Bamford et al. 2004; Fukushima et al. 2014; Wang et al. 2014; Ichimura et al. 2016).This mutation leads to an amino acid charge alteration at a critical position for the guanosine triphosphate hydrolysis reaction. In addition, NIH3T3 cells overexpressing KRAS p.E63K mutation showed altered morphology and displayed higher proliferative and migratory rates (Angeles et al. 2019). Interestingly, some cases of KRAS mutations have been reported as teratoma with adenocarcinoma transformation. However, this mutation is observed in both benign intestinal-type epithelium and adenocarcinoma component of the teratoma, suggesting that it is an early event in the carcinogenic sequence (Hershkovitz et al. 2013; Li et al. 2014; Kim et al. 2015). The third common mutation is the p.S447P mutation in the ATPase domain of the POLQ DNA double strand repair enzyme known to participate in cancer progression and resistance to therapy (Schrempf et al. 2021). Interestingly, two studies have shown that mutations in this domain may lead to its inactivation and thereby impact the sequence of the repaired products (Wyatt et al. 2016; Zahn and Jensen 2021). Although, the SIFT and PolyPhen prediction tools indicate a deleterious impact of the p.S447P mutation on protein function, additional data are needed to definitively confirm its potential involvement in the mutagenesis process.

GSEA showed an enrichment of the mutated genes in the melanoma pathway. The four genes (*KRAS*, *TP53*, *ERBB4*, and *KDR*) driving this enrichment are recognized for their implication as Cancer Census genes according to the COSMIC database (Bamford et al. 2004). This result is in accordance with the histologic findings showing that the anaplastic transformation of the MNT is histologically close to a malignant melanoma and expresses melanocytic protein markers SOX10, Melan-A, and HMB45. TP53 and KRAS are oncoproteins which have been described as potentially involved in melanoma (Cicenas et al. 2017; Hayward et al. 2017). In addition, mutations of ERBB4 and KDR have also been described in melanoma and these mutations are significantly more present in tumors with any known recurrent mutations in classical driver genes including *BRAF*, *NRAS*, *KIT*, *GNAQ*, and *GNA11* (Xia et al. 2014). ERBB4 is a member of EGFR subfamily of receptor tyrosine kinase containing well-known EGFR and HER2 oncoproteins. In our study, we observed a p.A972V ERBB4 variant present specifically in the anaplastic MNT component. This mutation has not been previously described as a classical hotspot mutation in the protein but it is located in the intracytoplasmic tyrosine kinase domain, which is classically mutated in cancer development (Lucas et al. 2022). We also observed a somatic variant in the intracytoplasmic domain of KDR (p.T1258M), also known as VEGFR2, which is specific to the anaplastic MNT component. Altogether, these results suggest a potential involvement of these four variants in the development of the anaplastic MNT transformation of the teratoma.

METHODS

Patient and Samples

The different samples were collected at the Oncology department of Strasbourg University Hospitals and analyzed at the Pathology department. The research protocol was approved by the institutional review board of Strasbourg University Hospitals, and a written informed consent was obtained from the patient. Samples were collected and processed under the principles of the Helsinki declaration. Tissue samples for histopathologic analysis were immediately fixed in 4% neutral buffered formalin for 24 h and processed according to standard procedures on slides stained with haematoxylin and eosin (H&E) method. All relevant pathology materials were carefully reviewed by expert pathologists. The tumor cellularity was 40% for the teratoma and 60% for the MNT and the anaplastic MNT.

Immunohistochemistry and In Situ Hybridization Studies

Immunohistochemical studies were performed on formalin-fixed paraffin-embedded (FFPE) sections following routine protocols on a Ventana Benchmark XT automated slide stainer (Ventana). An extensive antibody panel—which included the following antibodies—was used for diagnostic purposes: PS-100 (clone EP-32), SOX10 (clone EP268), Melan-A (clone A103), HMB45 (clone MO634), glypican 3 (clone GC33), bHCG (clone CGO4/CGO5), synaptophysin (Clone 27G12), panKeratin AE1/E3 (clone AE1 + AE3), and SALL4 (clone 6E3).

Targeted Panel Sequencing

DNA was extracted from FFPE tissue sections using the QIAamp DNA FFPE Tissue Kit (QIAGEN) or the Maxwell 16 FFPE Plus LEV DNA Purification Kit (Promega), respectively, and according to the manufacturers' recommendations. Targeted sequencing was made only on anaplastic NMT FFPE sample within the routine clinical care process in order to identify potential therapeutic targets. Libraries were prepared with the Multiplicom Tumor Hotspot MASTR Plus kit (Agilent) covering hotspot mutations in 26 genes validated by the French Cancer Institute (INCa). The list of analyzed genes and exons is as follows: *AKT1* (exon 3), *ALK* (exons 20–29), *BRAF* (exons 11–15), *CDKN2A* (complete coding sequence), *CTNNB1* (exon 3), *DDR2* (complete coding sequence), *EGFR* (exons 18–21), *ERBB2* (exons 19–21), *ERBB4* (exons 10 and 12), *FGFR2* (exons 7, 12, and 14), *FGFR3* (exons 7, 9, 14, and 16), *H3F3A* (exon 2), *HIST1H3B* (exon 1), *HRAS* (exons 2–4), *IDH1* (exon 4), *IDH2* (exon 4), *KIT* (exons 8–11, 13–14, and 17–18), *KRAS* (exons 2–4), *MAP2K1/MEK1* (exons 2–3), *MET* (exons 2, 10, and 14–20), *NRAS* (exons 2–4), *PDGFRA* (exons 12, 14, and 18), *PIK3CA* (exons 2–3, 10–11, and 21), *PIK3R1* (exons 11–13), *PTEN* (complete coding sequence), and *STK11/LKB1* (complete coding sequence). Sequencing libraries were prepared with the SureSelectQXT Target Enrichment System kit (Agilent Technologies) following the manufacturer's instructions and sequenced on an Illumina MiSeq instrument (Illumina) (Okutman et al. 2021). Bioinformatics analysis was performed using STARK (version 0.9b), as previously described (Okutman et al. 2021). Only nonsilencing variants with an allelic frequency of >4% and a sequencing depth of >300 reads were reported.

Exome Sequencing

Exome sequencing was performed on four FFPE samples including mature teratoma, MNT, metastatic anaplastic MNT component, and a matched germline thymic sample serving as a nontumoral control. The purification of genomic DNA was performed with the GeneRead DNA FFPE kit (QIAGEN) according to the manufacturer's instructions. The genomic DNA was quantified using a Qubit instrument and the dsDNA BR Assay kit (Thermo Fisher Scientific). Exome sequencing libraries were prepared with the Twist Human Core Exome

Kit (Twist Bioscience) following the manufacturer's recommendations. Paired-end (2-bp × 75-bp) sequencing was performed on a NextSeq500 sequencer (Illumina) with an average depth of coverage of 317.5, 405, 194.4, and 172 for the mature teratoma, MNT, metastatic MNT, and matched germline thymic samples, respectively. Sequences were mapped to the hg19 reference genome using BWA v0.7.17 (Li and Durbin 2010). Sequence variants were called using the GATK mutect2 v4.1.8.0 and vardict v1.8.2 tools and only those with the "PASS" filter were considered (Cibulskis et al. 2013; Lai et al. 2016). Variants were annotated using VEP (version 94) (McLaren et al. 2016) and filtered as follows: depth of coverage in tumor and corresponding normal samples >10, depth of coverage of alternative bases in tumor ≥5 and in normal equal to 0, and VAF > 5%. Variants described in the 1000 Genomes Project and gnomAD database with an allele frequency of >1% were discarded. We focused only on protein-altering variants (missense, nonsense, splice site variants, start and stop gain/loss, and coding indels). Raw exome data (FASTQ files) are available at the National Center for Biotechnology Information's Sequence Read Archive (accession PRJNA825743).

For GSEA, we defined a score for each gene carrying a somatic coding or splice site variant. This score was defined as the weighted sum of conditions in which this variant was found. Weights were chosen as 1, 2, and 3 for mature teratoma, MNT, and anaplastic MNT, respectively, as a gradation of their involvement in anaplastic transformation. This weighted gene list was then analyzed using the online WEB-based Gene Set Analysis toolkit for Human Transcriptome (www.webgestalt.org) and the WikiPathway database. Functional enrichment analyses were based on false discovery rate (FDR) < 0.05 and normalized enrichment score (NES) (Benjamini and Hochberg 1995; Subramanian et al. 2005).

ADDITIONAL INFORMATION

Data Deposition and Access

Raw exome data (FASTQ files) are available at the National Center for Biotechnology Information's Sequence Read Archive (accession: PRJNA825743). Variants of Table 1 are available in ClinVar (https://www.ncbi.nlm.nih.gov/clinvar/) under the accession numbers VCV000501513.5, VCV000017379.26, VCV000634705.4, and SCV003915799–SCV003915823.

Ethics Statement

The research protocol was approved by the institutional review board of Strasbourg University Hospitals, and a written informed consent was obtained from the patient.

Authors' Contributions

S.Ma., B.L., and R.C. designed research, performed research, and wrote the manuscript; J.G., A.M., T.S., S.Me, A.K., and J-E.K. analyzed data and reviewed the manuscript; and S.B. designed research and reviewed the manuscript.

Competing Interest Statement

The authors have declared no competing interest.

Referees

Katherine E. Miller
Anonymous

Received November 17, 2022; accepted in revised form April 11, 2023.

Funding

This work was supported by the Strasbourg's Interdisciplinary Thematic Institute (ITI) for Precision Medicine, TRANSPLANTEX NG, as part of the ITI 2021-2028 program of the University of Strasbourg, CNRS and INSERM, funded by IdEx Unistra [ANR-10-IDEX-0002] and SFRI-STRAT'US [ANR-20-SFRI-0012]; Institut National de la Santé et de la Recherche Médicale UMR_S 1109; MSD-Avenir grant AUTOGEN; the European Regional Development Fund (European Union) INTERREG V program PERSONALIS.

REFERENCES

Albany C, Einhorn LH. 2013. Extragonadal germ cell tumors: clinical presentation and management. *Curr Opin Oncol* **25:** 261–265. doi:10.1097/CCO.0b013e32835f085d

Almomani MH, Rentea RM. 2022. *Melanotic neuroectodermal tumor of infancy*. StatPearls, Treasure Island, FL.

Anagnostaki L, Krag Jacobsen G, Horn T, Sengelov L, Braendstrup O. 1992. Melanotic neuroectodermal tumour as a predominant component of an immature testicular teratoma. Case report with immunohistochemical investigations. *APMIS* **100:** 809–816. doi:10.1111/j.1699-0463.1992.tb04004.x

Angeles AKJ, Yu RTD, Cutiongco-De La Paz EM, Garcia RL. 2019. Phenotypic characterization of the novel, non-hotspot oncogenic KRAS mutants E31D and E63K. *Oncol Lett* **18:** 420–432. doi:10.3892/ol.2019.10325

Bamford S, Dawson E, Forbes S, Clements J, Pettett R, Dogan A, Flanagan A, Teague J, Futreal PA, Stratton MR, et al. 2004. The COSMIC (Catalogue of Somatic Mutations in Cancer) database and website. *Br J Cancer* **91:** 355–358. doi:10.1038/sj.bjc.6601894

Barrett AW, Morgan M, Ramsay AD, Farthing PM, Newman L, Speight PM. 2002. A clinicopathologic and immunohistochemical analysis of melanotic neuroectodermal tumor of infancy. *Oral Surg Oral Med Oral Pathol Oral Radiol Endod* **93:** 688–698. doi:10.1067/moe.2002.124000

Benjamini Y, Hochberg Y. 1995. Controlling the false discovery rate: a practical and powerful approach to multiple testing. *J R Stat Soc Ser B Methodol* **57:** 289–300. doi:10.1111/j.2517-6161.1995.tb02031.x

Blanco L, Tirado CA. 2018. Testicular germ cell tumors: a cytogenomic update. *J Assoc Genet Technol* **44:** 128–133.

Chiang YT, Chien YC, Lin YH, Wu HH, Lee DF, Yu YL. 2021. The function of the mutant p53-R175H in cancer. *Cancers (Basel)* **13:** 16. doi:10.3390/cancers13164088

Cibulskis K, Lawrence MS, Carter SL, Sivachenko A, Jaffe D, Sougnez C, Gabriel S, Meyerson M, Lander ES, Getz G. 2013. Sensitive detection of somatic point mutations in impure and heterogeneous cancer samples. *Nat Biotechnol* **31:** 213–219. doi:10.1038/nbt.2514

Cicenas J, Tamosaitis L, Kvederaviciute K, Tarvydas R, Staniute G, Kalyan K, Meskinyte-Kausiliene E, Stankevicius V, Valius M. 2017. KRAS, NRAS and BRAF mutations in colorectal cancer and melanoma. *Med Oncol* **34:** 26. doi:10.1007/s12032-016-0879-9

Cooke SL, Ennis D, Evers L, Dowson S, Chan MY, Paul J, Hirschowitz L, Glasspool RM, Singh N, Bell S, et al. 2017. The driver mutational landscape of ovarian squamous cell carcinomas arising in mature cystic teratoma. *Clin Cancer Res* **23:** 7633–7640. doi:10.1158/1078-0432.CCR-17-1789

De Backer A, Madern GC, Pieters R, Haentjens P, Hakvoort-Cammel FG, Oosterhuis JW, Hazebroek FW. 2008. Influence of tumor site and histology on long-term survival in 193 children with extracranial germ cell tumors. *Eur J Pediatr Surg* **18:** 1–6. doi:10.1055/s-2007-989399

Dulmet EM, Macchiarini P, Suc B, Verley JM. 1993. Germ cell tumors of the mediastinum. A 30-year experience. *Cancer* **72:** 1894–1901. doi:10.1002/1097-0142(19930915)72:6<1894::AID-CNCR2820720617>3.0.CO;2-6

Feldman DR, Iyer G, Van Alstine L, Patil S, Al-Ahmadie H, Reuter VE, Bosl GJ, Chaganti RS, Solit DB. 2014. Presence of somatic mutations within PIK3CA, AKT, RAS, and FGFR3 but not BRAF in cisplatin-resistant germ cell tumors. *Clin Cancer Res* **20:** 3712–3720. doi:10.1158/1078-0432.CCR-13-2868

Fichtner A, Richter A, Filmar S, Gaisa NT, Schweyer S, Reis H, Nettersheim D, Oing C, Gayer FA, Leha A, et al. 2021. The detection of isochromosome i(12p) in malignant germ cell tumours and tumours with somatic malignant transformation by the use of quantitative real-time polymerase chain reaction. *Histopathology* **78:** 593–606. doi:10.1111/his.14258

Fukushima S, Otsuka A, Suzuki T, Yanagisawa T, Mishima K, Mukasa A, Saito N, Kumabe T, Kanamori M, Tominaga T, et al. 2014. Mutually exclusive mutations of KIT and RAS are associated with KIT mRNA expression and chromosomal instability in primary intracranial pure germinomas. *Acta Neuropathol* **127:** 911–925. doi:10.1007/s00401-014-1247-5

Green DB, La Rosa FG, Craig PG, Khani F, Lam ET. 2021. Metastatic mature teratoma and growing teratoma syndrome in patients with testicular non-seminomatous germ cell tumors. *Korean J Radiol* **22:** 1650–1657. doi:10.3348/kjr.2020.1391

Hameed K, Burslem MR. 1970. A melanotic ovarian neoplasm resembling the "retinal anlage" tumor. *Cancer* **25:** 564–567. doi:10.1002/1097-0142(197003)25:3<564::AID-CNCR2820250310>3.0.CO;2-L

Hayward NK, Wilmott JS, Waddell N, Johansson PA, Field MA, Nones K, Patch AM, Kakavand H, Alexandrov LB, Burke H, et al. 2017. Whole-genome landscapes of major melanoma subtypes. *Nature* **545:** 175–180. doi:10.1038/nature22071

Hershkovitz D, Vlodavsky E, Simon E, Ben-Izhak O. 2013. KRAS mutation positive mucinous adenocarcinoma originating in mature ovarian teratoma: case report and review of literature. *Pathol Int* **63:** 611–614. doi:10.1111/pin.12123

Ichimura K, Fukushima S, Totoki Y, Matsushita Y, Otsuka A, Tomiyama A, Niwa T, Takami H, Nakamura T, Suzuki T, et al. 2016. Recurrent neomorphic mutations of MTOR in central nervous system and testicular germ cell tumors may be targeted for therapy. *Acta Neuropathol* **131:** 889–901. doi:10.1007/s00401-016-1557-x

Kim ES, Kwon MJ, Song JH, Kim DH, Park HR. 2015. Adenocarcinoma arising from intracranial recurrent mature teratoma and featuring mutated KRAS and wild-type BRAF genes. *Neuropathology* **35:** 44–49. doi:10.1111/neup.12140

King ME, Micha JP, Allen SL, Mouradian JA, Chaganti RS. 1985. Immature teratoma of the ovary with predominant malignant retinal anlage component. A parthenogenically derived tumor. *Am J Surg Pathol* **9:** 221–231. doi:10.1097/00000478-198503000-00006

Lai Z, Markovets A, Ahdesmaki M, Chapman B, Hofmann O, McEwen R, Johnson J, Dougherty B, Barrett JC, Dry JR. 2016. VarDict: a novel and versatile variant caller for next-generation sequencing in cancer research. *Nucl Acids Res* **44:** e108. doi:10.1093/nar/gkw227

Larson RA. 2009. Therapy-related myeloid neoplasms. *Haematologica* **94:** 454–459. doi:10.3324/haematol.2008.005157

Lee T, Seo Y, Han J, Kwon GY. 2019. Analysis of Chromosome 12p over-representation and clinicopathological features in mediastinal teratomas. *Pathology* **51:** 62–66. doi:10.1016/j.pathol.2018.10.002

Li H, Durbin R. 2010. Fast and accurate long-read alignment with Burrows-Wheeler transform. *Bioinformatics* **26:** 589–595. doi:10.1093/bioinformatics/btp698

Li Y, Zhang R, Pan D, Huang B, Weng M, Nie X. 2014. KRAS mutation in adenocarcinoma of the gastrointestinal type arising from a mature cystic teratoma of the ovary. *J Ovarian Res* **7:** 85. doi:10.1186/s13048-014-0085-3

Lucas LM, Dwivedi V, Senfeld JI, Cullum RL, Mill CP, Piazza JT, Bryant IN, Cook LJ, Miller ST, Lott JH IV, et al. 2022. The Yin and Yang of ERBB4: tumor suppressor and oncoprotein. *Pharmacol Rev* **74:** 18–47. doi:10.1124/pharmrev.121.000381

Marei HE, Althani A, Afifi N, Hasan A, Caceci T, Pozzoli G, Morrione A, Giordano A, Cenciarelli C. 2021. p53 signaling in cancer progression and therapy. *Cancer Cell Int* **21:** 703. doi:10.1186/s12935-021-02396-8

Marx A, Chan JKC, Chalabreysse L, Dacic S, Detterbeck F, French CA, Hornick JL, Inagaki H, Jain D, Lazar AJ, et al. 2022. The 2021 WHO classification of tumors of the thymus and mediastinum: what is new in thymic epithelial, germ cell, and mesenchymal tumors? *J Thorac Oncol* **17:** 200–213. doi:10.1016/j.jtho.2021.10.010

McLaren W, Gil L, Hunt SE, Riat HS, Ritchie GR, Thormann A, Flicek P, Cunningham F. 2016. The ensembl variant effect predictor. *Genome Biol* **17:** 122. doi:10.1186/s13059-016-0974-4

Misugi K, Okajima H, Newton WA Jr, Kmetz DR, Delorimier AA. 1965. Mediastinal origin of a melanotic progonoma or retinal anlage tumor: ultrastructural evidence for neural crest origin. *Cancer* **18:** 477–484. doi:10.1002/1097-0142(196504)18:4<477::AID-CNCR2820180411>3.0.CO;2-N

Moran CA, Suster S. 1997. Primary germ cell tumors of the mediastinum: I. Analysis of 322 cases with special emphasis on teratomatous lesions and a proposal for histopathologic classification and clinical staging. *Cancer* **80:** 681–690. doi:10.1002/(SICI)1097-0142(19970815)80:4<681::AID-CNCR6>3.0.CO;2-Q

Motzer RJ, Amsterdam A, Prieto V, Sheinfeld J, Murty VV, Mazumdar M, Bosl GJ, Chaganti RS, Reuter VE. 1998. Teratoma with malignant transformation: diverse malignant histologies arising in men with germ cell tumors. *J Urol* **159:** 133–138. doi:10.1016/S0022-5347(01)64035-7

Okutman O, Tarabeux J, Muller J, Viville S. 2021. Evaluation of a custom design gene panel as a diagnostic tool for human non-syndromic infertility. *Genes (Basel)* **12:** 410. doi:10.3390/genes12030410

Oosterhuis JW, Stoop H, Honecker F, Looijenga LH. 2007. Why human extragonadal germ cell tumours occur in the midline of the body: old concepts, new perspectives. *Int J Androl* **30:** 256–263; discussion 263–254. doi:10.1111/j.1365-2605.2007.00793.x

Pini GM, Colecchia M. 2022. Mediastinal germ cell tumors: a narrative review of their traits and aggressiveness features. *Mediastinum* **6:** 5. doi:10.21037/med-21-22

Ronchi A, Cozzolino I, Montella M, Panarese I, Zito Marino F, Rossetti S, Chieffi P, Accardo M, Facchini G, Franco R. 2019. Extragonadal germ cell tumors: not just a matter of location. A review about clinical, molecular and pathological features. *Cancer Med* **8:** 6832–6840. doi:10.1002/cam4.2195

Ryu YJ, Yoo SH, Jung MJ, Jang S, Cho KJ. 2013. Embryonal rhabdomyosarcoma arising from a mediastinal teratoma: an unusual case report. *J Korean Med Sci* **28:** 476–479. doi:10.3346/jkms.2013.28.3.476

Schrempf A, Slyskova J, Loizou JI. 2021. Targeting the DNA repair enzyme polymerase theta in cancer therapy. *Trends Cancer* **7:** 98–111. doi:10.1016/j.trecan.2020.09.007

Smith MR, Neuberg D, Flinn IW, Grever MR, Lazarus HM, Rowe JM, Dewald G, Bennett JM, Paietta EM, Byrd JC, et al. 2011. Incidence of therapy-related myeloid neoplasia after initial therapy for chronic lymphocytic leukemia with fludarabine-cyclophosphamide versus fludarabine: long-term follow-up of US Intergroup Study E2997. *Blood* **118:** 3525–3527. doi:10.1182/blood-2011-03-342485

Styczewska M, Krawczyk MA, Brecht IB, Haug K, Izycka-Swieszewska E, Godzinski J, Raciborska A, Ussowicz M, Kukwa W, Cwalina N, et al. 2021. The role of chemotherapy in management of inoperable, metastatic and/or recurrent melanotic neuroectodermal tumor of infancy-own experience and systematic review. *Cancers (Basel)* **13:** 3872. doi:10.3390/cancers13153872

Subramanian A, Tamayo P, Mootha VK, Mukherjee S, Ebert BL, Gillette MA, Paulovich A, Pomeroy SL, Golub TR, Lander ES, et al. 2005. Gene set enrichment analysis: a knowledge-based approach for interpreting genome-wide expression profiles. *Proc Natl Acad Sci* **102:** 15545–15550. doi:10.1073/pnas.0506580102

Tamura R, Yoshihara K, Nakaoka H, Yachida N, Yamaguchi M, Suda K, Ishiguro T, Nishino K, Ichikawa H, Homma K, et al. 2020. XCL1 expression correlates with CD8-positive T cells infiltration and PD-L1 expression in squamous cell carcinoma arising from mature cystic teratoma of the ovary. *Oncogene* **39:** 3541–3554. doi:10.1038/s41388-020-1237-0

Tamura R, Nakaoka H, Yachida N, Ueda H, Ishiguro T, Motoyama T, Inoue I, Enomoto T, Yoshihara K. 2023. Spatial genomic diversity associated with APOBEC mutagenesis in squamous cell carcinoma arising from ovarian teratoma. *Cancer Sci* doi:10.1111/cas.15754

Taylor-Weiner A, Zack T, O'Donnell E, Guerriero JL, Bernard B, Reddy A, Han GC, AlDubayan S, Amin-Mansour A, Schumacher SE, et al. 2016. Genomic evolution and chemoresistance in germ-cell tumours. *Nature* **540:** 114–118. doi:10.1038/nature20596

Timmerman DM, Eleveld TF, Gillis AJM, Friedrichs CC, Hillenius S, Remmers TL, Sriram S, Looijenga LHJ. 2021. The role of TP53 in cisplatin resistance in mediastinal and testicular germ cell tumors. *Int J Mol Sci* **22:** 11774. doi:10.3390/ijms222111774

Tobo M, Sumiyoshi A, Yamakawa Y. 1981. Sellar teratoma with melanotic progonoma. A case report. *Acta Neuropathol* **55:** 71–73. doi:10.1007/BF00691534

Vajtai I, Sutak I, Varga Z. 2000. Melanotic progonoma as a component of ovarian teratoma. *Histopathology* **36:** 283–285. doi:10.1046/j.1365-2559.2000.0872d.x

Wang L, Yamaguchi S, Burstein MD, Terashima K, Chang K, Ng HK, Nakamura H, He Z, Doddapaneni H, Lewis L, et al. 2014. Novel somatic and germline mutations in intracranial germ cell tumours. *Nature* **511:** 241–245. doi:10.1038/nature13296

Wyatt DW, Feng W, Conlin MP, Yousefzadeh MJ, Roberts SA, Mieczkowski P, Wood RD, Gupta GP, Ramsden DA. 2016. Essential roles for polymerase theta-mediated end joining in the repair of chromosome breaks. *Mol Cell* **63:** 662–673. doi:10.1016/j.molcel.2016.06.020

Xia J, Jia P, Hutchinson KE, Dahlman KB, Johnson D, Sosman J, Pao W, Zhao Z. 2014. A meta-analysis of somatic mutations from next generation sequencing of 241 melanomas: a road map for the study of genes with potential clinical relevance. *Mol Cancer Ther* **13:** 1918–1928. doi:10.1158/1535-7163.MCT-13-0804

Zahn KE, Jensen RB. 2021. Polymerase theta coordinates multiple intrinsic enzymatic activities during DNA repair. *Genes (Basel)* **12:** 1310. doi:10.3390/genes12091310

Zhang C, Zhou X, Huang X, Ding X, Wang Y, Zhang R. 2022. Genomic characterization of intracranial teratomas using whole genome sequencing. *Front Oncol* **12:** 1013722. doi:10.3389/fonc.2022.1013722

Genomic profiling of a metastatic anaplastic melanocytic neuroectodermal tumor arising from a mature thymic teratoma as part of a mediastinal germ cell tumor

Sylvain Mayeur, Benoit Lhermitte, Justine Gantzer, et al.

Cold Spring Harb Mol Case Stud 2023, **9:** a006257
Access the most recent version at doi:10.1101/mcs.a006257